IJCSI International Journal of Computer Science Issues, Volume 13, Issue 5, September 2016
ISSN (Print): 1694-0814 | ISSN (Online): 1694-0784
www.IJCSI.org https://doi.org/10.20943/01201605.135145

Numerical study on Optimization of key parameters for better cutting performance of shield machine cutters

TAN Qing[1, 3], YI Nian-en[1, 2,*], XIA Yi-min[1, 2], ZHU Yi [2], YI Liang [1, 2], YIZENG Siyuan [2]

[1.]State Key Laboratory of High Performance Complex Manufacturing, Central South University, Changsha, Hunan 410083, China

[2.]School of Mechanical and Electrical Engineering, Central South University, Changsha, Hunan 410083, China

[3.]Light Alloy Institute, Central South University, Changsha, Hunan 410083, China

Abstract

In order to improve the cutting performance of shield machine disc cutters (short for cutters), penetration depth (denoted as *p*) and cutting spacing (denoted as *s*) were selected as key optimization parameters. Cutting forces and the area of crushing pits were used as performance indices. To analyze the influence of the parameters on the cutting performance of the cutters, a three-dimensional finite element model was established which was verified by a well-known theoretical model. Using this model, the rock-cutting processes in relieved (double-cutter-cutting) and unrelieved (single-cutter-cutting) modes were numerically simulated to get the cutting forces and the area of crushing pits. The regression equation based on these key parameters was built. The research shows that increasing penetration depth would help improve the work ratio done by the rolling force but may cause greater vibration and impact when the cutters are being used in the unrelieved mode. With the increasing of the penetration depth, the area of crushing pits rises. In relieved mode, when *s/p* is smaller than 10, the forces of cutters and the area of crushing pits rapidly increase with the increasing of cutting spacing. In this case, increasing cutting spacing is a good choice for better cutting efficiency. However, when *s/p* is greater than 10 and less than 16, the area of crushing pits decrease and the rolling force is no longer sensitive to the increasing of cutting spacing. When *s/p* is greater than 16, the cutting spacing has little influence on the area of crushing pits.

Keywords: *disc cutter; cutting force; cutting spacing; penetration depth; cutting performance; performance optimization*

1. Introduction

With the development of tunnel engineering [1],[2], shield tunneling machines (short for shield machines) have been widely used because of their great advantages such as high tunneling efficiency, high security and low noise [3],[4]. As the key parameters of shield machine disc cutters (short for cutters), penetration depth and cutting spacing have significant influence on cutting efficiency, cutters lifetime, the design quality of shield machine cutterheads and construction progress. There are many scholars who are trying to identify key influence parameters of cutters. For example, according to the pressure distribution between cutters and rocks, a well-known cutting force prediction model was established by Rostami and Ozdemir[5],[6]. The influence of *s/p* on cutting forces and cutting performance are systematically studied in a linear cutting test with multiple geological conditions by Gertsch etc.[7]. By carrying out a granite-cutting experiment on a linear cutting test platform, Cho etc.[8] believed that coupling effects of adjacent cutters diminish when *s/p* is greater than 15. Chang etc.[9] also carried out a granite-cutting experiment with a 17 inches cutter and noted that the cutting efficiency may reach the peak

when *s/p* was between 10 and 12. However, the randomness of rock mechanics such as rock internal defects may incur undesirable results like the high prediction error. Moreover, some other models could well predict cutting forces but fail to calculate the area of rock crushed pits.

With the progress of computer, some researchers start to use the 2D numerical simulation technologies instead of rock cutting experiments to study rock-cutting processes of TBM cutters. By using UDEC 2D, Bejari H etc. [10],[11] studied the influence of joint on rock-cutting performance and the result shows that the increasing of joint spacing would decrease cutting rate of cutters. By utilizing the same software, Gong Q M etc.[12],[13] analyzed the rock-cutting processes with different joint characteristics. Liu J etc.[14],[15],[16] researched the penetration efficiency and rock crack propagation when single or double cutters are penetrating rocks with rock joints by using PFC2D. Huo J Z etc. [17] established the mapping relation between phase angles of adjacent cutters cutting rock in sequence and rock-breaking energy by employing RFPA2D. Liang Z Z etc.[18] numerically studied the emergence and development processes of rock crack under the action of different indenters. The above research shows that these 2D numerical methods can vividly and precisely reproduce the rock-cutting process of shield machine cutters at low costs, and therefore became an attractive alternative to cutting experiments. However, 2D numerical simulation models can hardly simulate the 3D rock-breaking process cutters. As a result of this disadvantage, it's difficult to obtain rock breaking volume by using these models.

This paper adopted ANSYS to build 3D finite element method (short for 3D FEM) to simulate rock-cutting process. The highlights of this paper are that a 3D rock-cutting numerical model was established through which the correlation curve between penetration depth and cutting forces in unrelieved mode was obtained. A cutting force regression model with respect to penetration depth was then established. Similarly, based on the calculation of cross-section area of debris, a rock-breaking volume regression model with respect to penetration depth was developed. The correlation curves between cutting spacing and cutting forces were obtained by simulating the rock-breaking process of cutters in relieved mode. Similarly, a cutting force regression model and a rock-breaking volume regression model were proposed for cutters used in relieved mode. Comparing cutting forces obtained from the simulation method with cutting forces predicted by the well-known theoretical model mentioned above, the 3D FE model was verified. The rock-breaking volume could be obtained from this 3D simulation model, which could be further used to assess tunneling efficiency.

2. Numerical modeling of rock-breaking process of cutters

A disc cutter with a constant cross-section (short for CCS cutter)is selected to build a 3D model, as shown in Fig. 1(top). The sectional dimension of its cutter ring is shown in Fig. 1(bottom). During the cutting process, the cutter is subjected to vertical force F_N, rolling force F_R and lateral force F_S which are three mutually perpendicular cutting force. These three-direction forces are provided by the thrust of the cutterheads, by the torque of the cutter, and by squeezing pressure of the rock and the centrifugal force of the revolutions of the cutterheads.

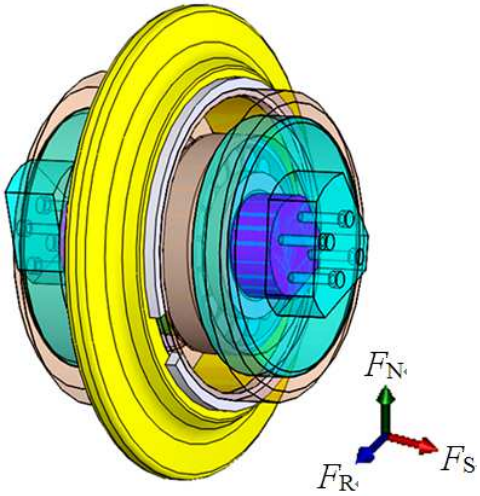

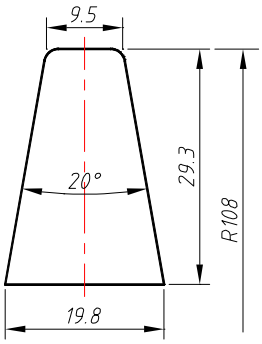

Fig. 1 The cutting forces of a disc cutter (top) and the sectional dimension of its cutter ring (bottom).

As shown in Fig. 2, installation radius of the cutter on the cutterhead is set to 1000mm; geometric dimensions of cross-section of the rock specimen is set to 100mm wide, and 30mm thick. The central angle of the specimen is set to 20°.

In order to save the computing time, the cutter is simplified and only the geometry model of its cutter ring is meshed with hexahedral elements. The mesh of the contact area between the cutter ring and rock is encrypted and refined. The 3D FE model obtained by meshing is shown in Fig. 2. The total number of nodes is 176425 and the number of elements is 152970.

Fig. 2 3D finite element model of rock-breaking of a cutter

The cutting process of shield machine cutters is complex and dynamic due to geometric nonlinearity, material nonlinearity, and contact nonlinearity and so on. In this paper, LS-DYNA program package is used to solve the finite element problem. The contact between the cutter and rock can be treated as a surface contact problem between a rigid body and a deformable body. During the rock-breaking process, some rock elements underneath the cutter ring keep failing, which will enable the other rock elements to be constantly in contact with the cutter blade. Therefore, the erosion surface to surface contact (ESTS) algorithm is adopted to simulate the failure process of rock elements.

The radial displacement of the ring along its own axis is constrained. So the cutter ring can rotate around this axis only when the friction produced on the surface between rock surface and cutter is sufficient. The friction coefficient is set to 0.3. No reflection boundary constrain is applied to all surfaces of the rock specimen except the top one and only the bottom surface is fully constrained. Lagrange algorithm is employed to simulate the penetration collision of nonlinear material and the deformation of the rock mesh. At the same time, the standard hourglass viscous damping algorithm is used to control the serious distortion of themes hand hourglass viscous damping coefficient is set in the range of 0.05 ~ 0.15. The cutter ring is defined as a rigid body. Select the *MAT_RIGID card to reduce the time of model calculation. According to the stress-strain characteristics of brittle rock, a dynamic damage constitutive model based on Ottosen four-parameter failure criterion is adopted which can be expressed as the follow formula:

$$\sigma^* = \left[A(1-D) + BP''^{Nf} \right]\left[1 + Cz\, ln\left(\varepsilon^*\right)\right] \quad (1)$$

Where the standard equivalent stress $\dot{\sigma}^*$ is defined as

$$\dot{\sigma}^* = \sigma^* / f_C^{'}.$$

$$D = \sum \frac{\Delta\varepsilon_p + \Delta\mu_p}{D_1\left(P'' + T''\right)^{D_2}} \quad (2)$$

Where, $T'' = Tp/f_c^{'}$.

The main material parameters of the cutter ring and rock are shown in Table 1 and Table 2 respectively. JHC constitutive model parameters are shown in Table 3. By changing the cutter spacing, penetration depth, a series of 3D FE model with different working conditions can be established and then solved using our high performance computing platform.

According to the above constitutive model, the fracture

and failure process of rock can be divided into three stages, as shown in Fig. 3.In the first stage, the elastic deformation takes place, followed by the plastic deformation stage. The last stage is the fracture damage stage.

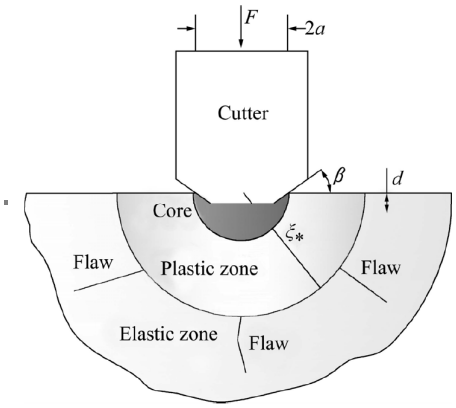

Fig. 3 Relationship of pressure and volumetric strain[15]

Table 1 Main material parameters of cutter ring

parameters	*units*	*value*
ρ	Kg/m^3	7900
E	GPa	206
v		0.3

Table 2 Main material parameters of rock

parameters	*units*	*value*
ρ	Kg/m^3	2450
E	GPa	1.88
v		0.23
σ_c	MPa	30.00
σ_t	MPa	1.36

Table 3 Parameters in JHC constitutive model

parameters	*units*	*value*
ρ	Kg/m^3	2450
G	GPa	0.76
A		0.79
B		1.60
Cz		0.007
Nf		0.61
fc'	MPa	30.0
Tp	MPa	1.36
$Smax$		7.0
$EFmin$		0.01
$Pcrush$	MPa	10.0
$\mu crush$		0.001
$Plock$	MPa	800
$\mu lock$		0.1
$D1$		0.04
$D2$		1.0
$K1$	GPa	85
$K2$	GPa	171
$K3$	GPa	208
Fs		1

3. Simulation analysis of rock-breaking process

As shown in Fig. 4, the rock-breaking process of a single cutter in unrelieved mode is simulated where set p is 4mm. It can be seen that the cutter ring is rolling over the rock along an arc track, rotating around Z axis and its own axis with the constrained radius. When the ring is rolling forward, the range of stress field in front of the blade spread forward and downward. Meanwhile, the contacting zone of rock with the blade is deformed. Once the stress in this zone exceeds the yield limit of rock material, elements with excessive deformation will be automatically deleted and finally there will be a cutting groove left on the rock surface. The width of groove is slightly larger than the width of the blade, Groove depth is slightly greater than the penetration depths shown in Fig. 5. The volume of crushing rock can be obtained by calculating the area of the crushing pit and cutting distance.

Cutting forces obtained by simulation is shown in Fig. 6. It can be seen that the magnitude of the rolling force the cutter bears is much smaller than that of the vertical force. Besides, the changing range of vertical forces is much greater than horizontal forces. During the cutting process, rolling force mainly contributes to the cutting work. In relieved mode, two adjacent cutters cut rock in consequence. Stress field produced by each cutter couples to each other. Finally, when the lateral cracks propagating underneath each cutter is overlapping. Major debris can be produced between the two slots. It can be seen from Fig. 7 that the area of crushing pits in relieved mode is generally greater than twice of the area

in unrelieved mode, which means that the relieved mode has higher efficiency than unrelieved mode.

Fig. 4 Rock-breaking process of a cutter working in unrelieved mode (unit: Pa)

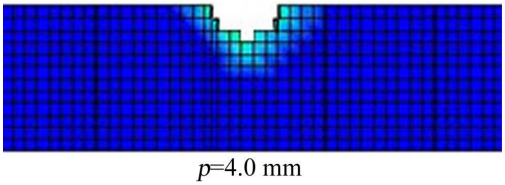

Fig. 5 Cross-sectional view of crushing pits

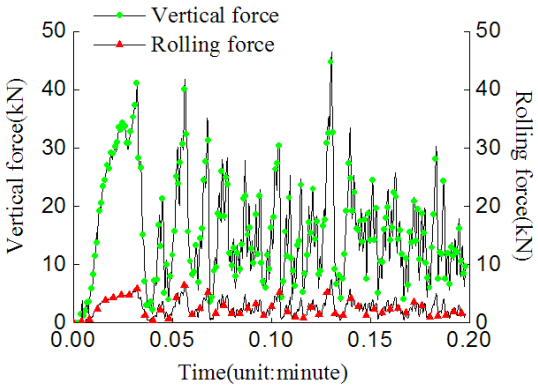

Fig. 6 Cutting forces obtained by simulation

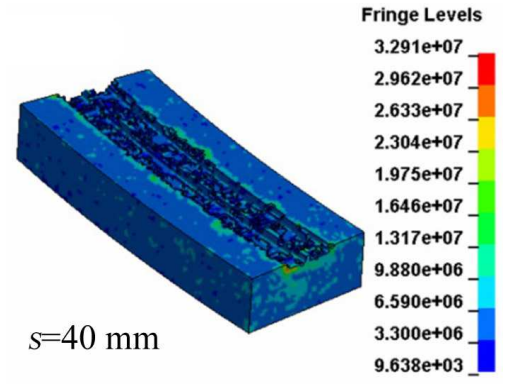

Fig. 7 Rock-breaking process of the double cutters working in relieved mode (unit: Pa)

4. Establishment of a theoretical model for predicting cutting forces

In order to verify the above FE model, the cutting forces obtained by simulation are compared with the forces calculated by the well-known theoretical model[5],[6], namely Rostami model in this paper. The contact pressure distribution between the cutter and rock is shown in Fig. 8.

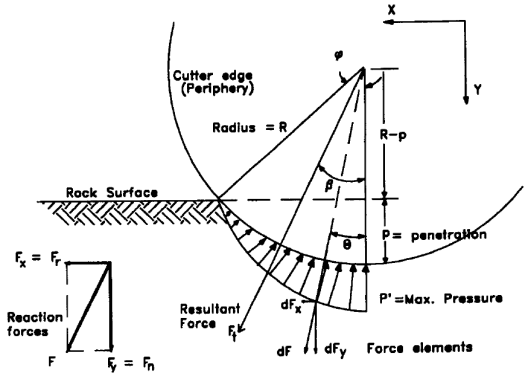

Fig. 8 Pressure distribution between a disc cutter and rock [5],[6]

The resultant force of the vertical force and the rolling force is directly given as follows:

$$F_t = \int_0^{\phi} TRPd\theta = \int_0^{\phi} TRP^0 \left(\frac{\theta}{\phi}\right)^{\psi} = \frac{TRP^0\phi}{1+\psi} \quad (3)$$

where,

$$P' = P^0 \left(\frac{\theta}{\phi}\right)^{\psi} \quad (4)$$

$$\phi = \cos^{-1}\left(\frac{R-p}{R}\right) \quad (5)$$

After analyzing the experimental data by logistic regression and dimensional analysis, we can get the basic pressure of the crushed zone,

$$P^0 = C_3\sqrt{\frac{s}{\phi\sqrt{RT}}\sigma_c^2\sigma_t} \quad (6)$$

Thus we get the vertical force F_N and the rolling force F_R which apply to the cutter ring. The two forces can be expressed as follow:

$$\begin{cases} F_N = F_t \cos(\beta) = C \dfrac{TR\phi}{1+\psi} \sqrt[3]{\dfrac{s\sigma_c^2 \sigma_t}{\phi\sqrt{RT}}} \cos(\gamma) \\ F_R = F_t \sin(\beta) = C \dfrac{TR\phi}{1+\psi} \sqrt[3]{\dfrac{s\sigma_c^2 \sigma_t}{\phi\sqrt{RT}}} \sin(\gamma) \end{cases} \quad (7)$$

The cutting coefficient is,

$$CC = \frac{F_R}{F_N} = \tan\gamma \quad (8)$$

For the cutter with a constant cross section, we assume that it has an approximately linear load distribution. If ψ=0, we can get,

$$CC = \frac{F_R}{F_N} = \frac{1-\cos\phi}{\sin\phi} = \tan\frac{\phi}{2} \quad (9)$$

Thus, we obtain the vertical force F_N and the rolling force F_R, which is acting on the cutter with a constant cross section,

$$\begin{cases} F_N = F_t \cos(\dfrac{\phi}{2}) = TR\phi P^0 \cos(\dfrac{\phi}{2}) \\ F_R = F_t \sin(\dfrac{\phi}{2}) = TR\phi P^0 \sin(\dfrac{\phi}{2}) \end{cases} \quad (10)$$

5. Influence of penetration depth on the cutting performance

The 3D FE model with difference penetration depth are solved and the volume of debris is calculated by the area of crushing pits. From Fig. 9, it can be seen that p=12mm has more the area of crushing pits than p=8mm. The height of the area of crushing pits has a linear relationship with the penetration depth. Shear forces acting on the rock debris by both sides of the cutter continuously increase as the penetration depth increase. Moreover, the deeper the depth is, the wider the bottom of the crushing pit is. However, the bottom width of the crushing pit is almost identical with the width of the blade. The stress zone produced underneath the cutter ring significantly expands and its value also rise with the increasing of penetration depth.

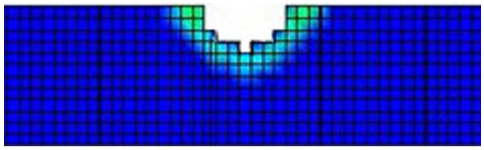

p=8.0 mm

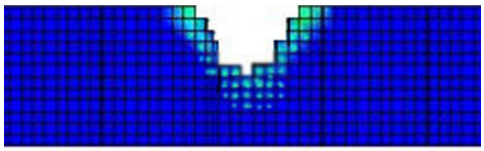

p=12.0 mm

Fig. 9 Cross-section view of two crushed pits.

The variation laws of cutting forces upon penetration depth are obtained by statistically analyzing the mean values of vertical force (Fig. 10) and rolling force (Fig. 11) under different sets of penetration depth calculated by the mentioned 3D FE model.

With the increase of penetration depth, both the vertical force and the rolling force increase proportionally. Since the work done by vertical force only account for 5% of total energy [19], the lower the ratio of the vertical force to the rolling force is, the better the cutting process is. Comparing Fig. 10 with Fig. 11, it can be seem that the vertical force is about 20 times as much as the rolling force when penetration depth is equal to 2mm, and becomes about 5 times when penetration depth is 12mm.It can be inferred that increasing the penetration depth can help improve the work done by the rolling force. According to the regression equations of the vertical force Eq.(11) and the rolling force Eq.(13), vertical force rise more rapidly than the rolling force dose along with the increase of penetration depth, which will lead to much more dynamic vibration acting on the cutter. Thus, in order to ensure the strength and reliability of the cutter, according to the given rotate speed and geological condition, the value of penetration depth must be set within a reasonable range. By comparing the simulation result with the theoretical one obtained by Rostami prediction model Eq.(10), it can be seen that the regression equations of the vertical force with respect to the penetration depth Eq. (11) and Eq. (12) has the same tendency as these of the rolling force Eq. (13) and Eq. (14), which validate the simulation results.

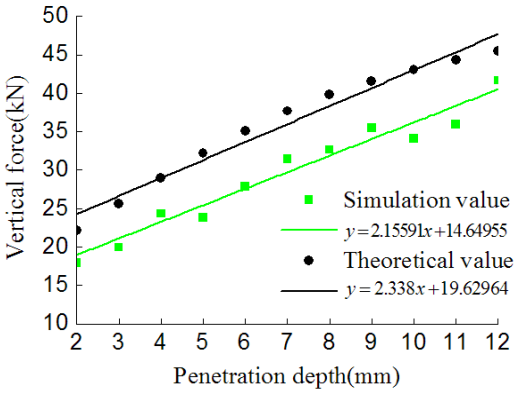

Fig. 10 The relationship between the vertical force and the penetration depth

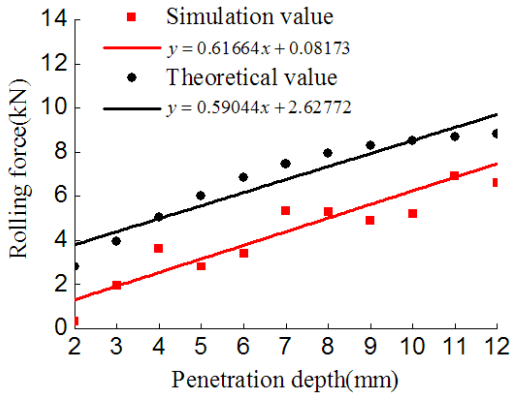

Fig. 11 The relationship between the rolling force and the penetration depth

The linear regression equation of the vertical force obtained by simulation with respect to the penetration depth is expressed as follow

$$y = 2.15591x + 14.64955 \quad (11)$$

The equation of the theoretical vertical force is:

$$y = 2.338x + 19.62964 \quad (12)$$

The equation of the simulated rolling force is:

$$y = 0.61664x + 0.08173 \quad (13)$$

The equation of the theoretical rolling force:

$$y = 0.59044x + 2.62772 \quad (14)$$

Base on the rock-breaking planar model perpendicular to the X axis, the area of crushing pits is calculated under different sets of penetration depth. The relationship between the area and the penetration depth can be obtained (Fig. 12).A fit linear equation was obtained as shown in Eq.(15). From this equation, it can be seen that the area of crushing pits increases with the increase of penetration depth. But the tendency reflected in the above relationship is less obvious. As the magnitude of the impact caused by the vertical force linearly increased with the increase of the penetration depth, we cannot blindly increase the penetration depth to raise the volume of crushing pits.

$$y = -9.088 + 16.142x \quad (15)$$

Assuming that the rolling distance of the cutter is l, the rock breaking volume is calculated by $V = yl$.

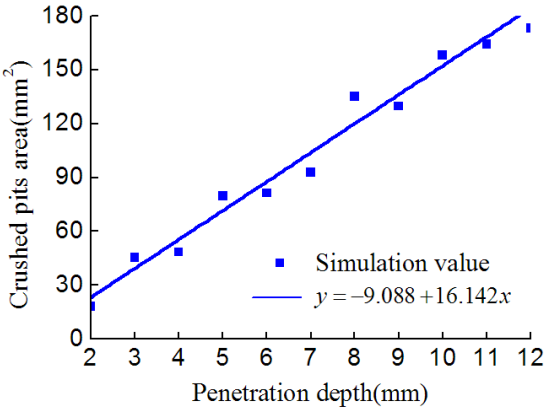

Fig. 12 The relationship between the area of crushing pits and the penetration depth

6. Influence of the cutting spacing on the cutting performances of the cutter

Set the penetration depth as p=8.0mm. The effects of different cutting spacing are shown in Fig. 13. When s=40mm, the two adjacent cutters are too close to work efficiently. The rock between the cutting grooves is over crushed and therefore the cutting efficiency is low. When s=60mm, the Mises stress in rock near one side of the cutting groove is huge. Rock cracks deeply extend inwards, which causes small fragments with smooth crushing surfaces near the rock surface. In this case, the cutting efficiency is improved. When s=80mm, the cutting spacing is too large to make cracks deep in rock overlap each other and therefore a small ledge appears on the rock fracture surface between the two cutting grooves. When s=100mm, the effects of the first cutting

groove on the second cutter is reduced and therefore an obvious ledge can be observed on the rock fracture surface between the cutting grooves. It can be concluded that, in order to improve the rock-breaking efficiency, the cutting spacing should be reasonably chosen to make the rock cracks overlap each other in a certain depth of rock, which could lead to large rock fragments.

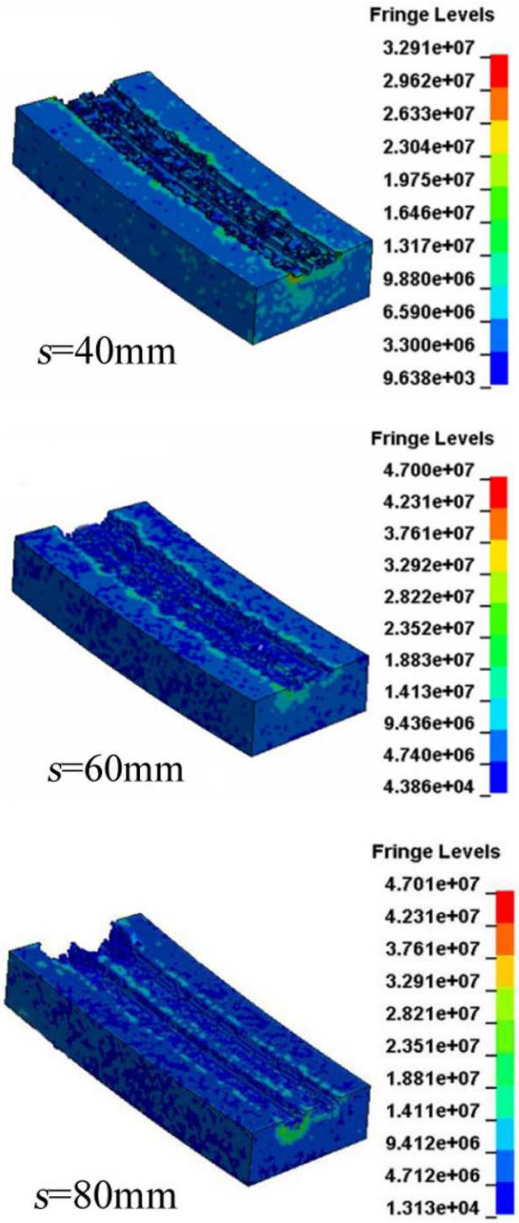

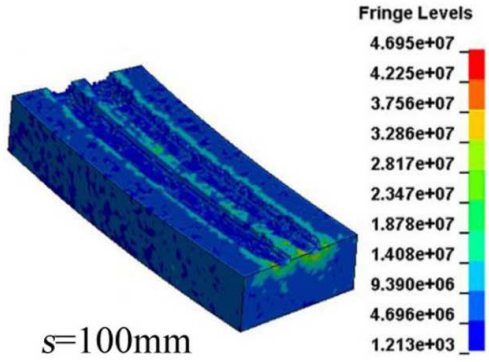

Fig. 13 Effects of the double cutters working in relieved mode (unit: Pa)

By statistically analyzing simulation results of the average vertical force (Fig. 14) and average rolling force (Fig. 15) under different sets of cutting spacing, the changing rule of the cutting forces with regards to the cutting spacing can be obtained. With the increase of the distance between the two cutters, the average values of the vertical force and rolling force exponentially increase. When $s/p<10$, with the increase of the cutting spacing, the cutting forces increase by a large margin. The rapid increase of the rolling force causes the rock breaking work grow, which helps improve the cutting efficiency. When $s/p>10$, the vertical force and rolling force increase slowly and therefore the changing cutting spacing has little effect on the rock-breaking process. The simulation results are compared with the cutting forces obtained by Rostami model, Eq. (10). It finds out that the regression equations Eq. (16) and Eq. (17) have the same tendency, so do the regression equations Eq. (18) and Eq. (19). The simulation results are also proved to be reliable.

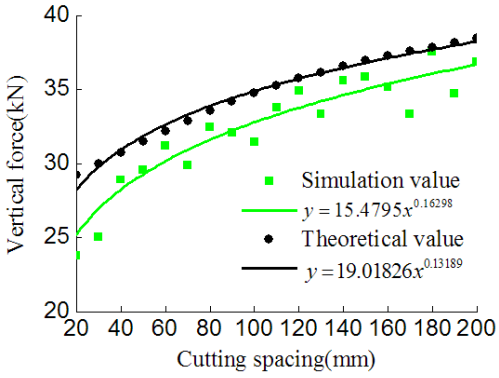

Fig. 14 The relationship between the vertical force and cutting spacing.

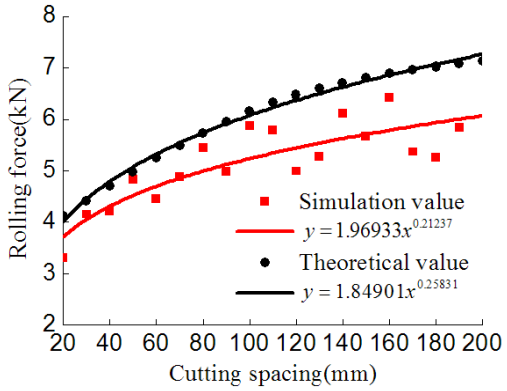

Fig. 15 The relationship between the rolling force and cutting spacing

The regression equation of the simulated vertical force with respect to the cutting spacing can be expressed as follow:

$$y=15.4795x^{0.16298} \quad (16)$$

The equation of the theoretical vertical force is:

$$y=19.01826x^{0.13189} \quad (17)$$

The equation of the simulated rolling force is:

$$y=1.96933x^{0.21237} \quad (18)$$

The equation of the theoretical rolling force:

$$y=1.84901x^{0.25831} \quad (19)$$

Through the 3D FE model, the area of crushing pits under different sets of cutter spacing is calculated. The relationship between the cutter spacing and the area is obtained, as shown in Fig. 16. To get the polynomial regression equation Eq. (20), regression analysis on the data points has been carried out. The results show that when s/p<10, the area of crushing pits increases rapidly with the increase of cutter spacing. The increase of cutter spacing would lead to the improvement of the cutting efficiency. When s/p>10, as the cutting spacing is greater than the length of propagated cracks. A ledge between the cutting grooves (Fig. 13 $s=100mm$) can be observed. Meanwhile, the area of crushing pits begins to decrease. When s/p>16, the cutting spacing doesn't seem to have powerful influence on the area of crushing pits. The crushed area is twice as much as the rock-breaking area produced by a single cutter.

$$y=100.3+8.9x-0.13x^2+0.00069x^3-0.00000127x^4 \quad (20)$$

Assuming that the rolling distance of the cutter is l, the volume of crushing pits is calculated by $V=yl$.

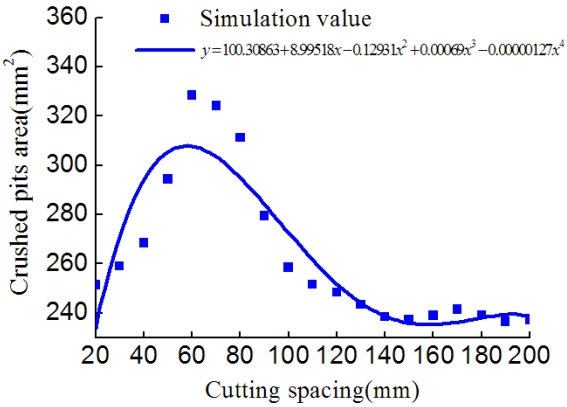

Fig. 16 The relationship between the cutting spacing and the area of crushing pits

7. Conclusions

In this paper, based on the constitutive characteristics of brittle rock materials. FE models of rock-cutting processes by shield machine cutters were established. Through the simulation, the relationship between penetration depth, cutting spacing, the area of crushing pits and cutting forces was obtained. The cutting efficiency of single and double cutters was evaluated respectively by calculating the area of crushing pits. The results of the study are listed as follows:

(1) In the single-cutter-cutting model, with the increase of penetration depth, the cutting work done by the rolling force which is treated as the effective component continues to increase. However, on the other hand, with the increase of penetration depth, the vertical force increases faster than the rolling force dose, which may cause the dynamic vibration. In order to ensure the strength and reliability of the cutter, penetration depth should be controlled within a reasonable range.

(2) In the double-cutter-cutting model, when s/p <10 with the increase of cutting spacing, the vertical force and the rolling force increase by a large margin. The increase of rolling force is beneficial to the improvement of rock-breaking work. When s/p >10,the vertical force

and rolling force grow slowly. In this case, changing the cutting spacing has no effect on the rock-breaking work.

(3) In the double-cutter-cutting model, when s/p <10 with the increase of cutting spacing, the area of crushing pits increases rapidly. The opposite tendency could be observed When s/p >10. When s/p >16, the cutting spacing has little effect on the area of crushing pits.

Notations

D= Damage factor
P= Actual pressure
P'' =Standard pressure
$\dot{\varepsilon}$ = Actual strain rate
$\dot{\varepsilon}^*$ = Dimensionless strain rate
$\dot{\varepsilon}_0$ = Reference strain rate
T'' = Standardization maximum static pressure
$F_{N=}$ The vertical force on disc cutter
$F_{R=}$ The rolling force on disc cutter
$F_{S=}$ The lateral force on disc cutter
s= Cutting spacing
p= Penetration depth
l = Rolling distance
V = Crushed pits volume
ρ= Material density
G= Shear modulus
A= Viscosity coefficient
B= Pressure enhancement factor
Cz= Strain rate coefficient
Nf= Pressure hardening index
fc'= Static yield strength of rock
Tp= Static tensile strength of rock
$Smax$= Maximum dimensionless strength coefficient of rock
$Pcrush$= Rock collapse point 1
$Plock$= Compaction pressure
$Mcrush$= Rock collapse point 2
$\mu lock$ = Volumetric strain of compaction point
$D1$= Material damage parameter 1
$D2$= Material damage parameter 2
EFmin= Material damage parameter 3
$K1$= Material pressure parameter 1
$K2$= Material pressure parameter 2
$K3$= Material pressure parameter 3
Fs= The failure type of rock
R= The radius of disc
T= Width of cutting edge
Ψ= Pressure distribution coefficient of cutting edge
ϕ = The contact angle between disc and rock
P'= The pressure of crushing zone
P^0= The basic pressure of crushing zone
σ_c= Compressive strength about rock
σ_t= Tensile strength about rock
E= Elastic modulus
v= Poisson ratio
C= Dimensionless coefficient (C≈2.12)
γ = The angle between the joint force of the disc cutter and the vertical center line of the disc cutter

Conflict of interest

The authors have confirmed that this article content has no conflict of interest.

Acknowledgment

This research was supported by National Program on Key Basic Research Project of China (2013CB035401); National Natural Science Foundation of China (51274252); National Natural Science Foundation of China (51074180).The authors would like to thank High Performance Computing Center of Central South University for their support in preparing this article.

References

[1] E. M. Abdelmoniem, and S. A. Mazen, and E. E: Hassanein "A framework for governance of post-construction activities in IS development projects (Case study in Egyptian environment)". International Journal of Computer Science Issues. Vol. 9, No. 5, 2012, pp.393-403.

[2] J. Sun, and P. Zhou, and Y. Wu: "Stress and wear analysis of the disc cutter of rock tunnel boring machine". Electronic Journal of Geotechnical Engineering. Vol. 9, No. 1, 2015, pp.721-725.

[3] A. Belghith, and S. B. H. Said, and B. Cousin: "Export

methods in fault detection and localization mechanisms" International Journal of Computer Science Issues, Vol. 9, No. 4, 2012, pp.463-471.

[4] S. B. Zheng, and S. P. Jiang: "Seismic resistance and damping model test and numerical simulation of highway tunnel". Open Civil Engineering Journal. Vol. 9, No. 1, 2015, pp.673-681.

[5] J. Rostami, and L. Ozdemir: "A new model for performance prediction of hard rock TBMs" Proceedings of Rapid Excavation and Tunnelling Conference(RETC). Boston, USA: [s. n.], 1993, pp.793-809.

[6] J. Rostami, and L. Ozdemir, and B. Nilson: "Comparison between CSM and NTH hard rock TBM performance prediction models" Proceedings of Annual Technical Meeting of the Institute of Shaft Drilling Technology. Las Vegas: [s. n.], 1996, pp.1-10.

[7] R. Gertsch, and L. Gertsch, and J. Rostami: "Disc cutting tests in Colorado red granite: Implications for TBM performance prediction" International Journal of Rock Mechanics and Mining Sciences, Vol. 44, No. 2, 2007, pp.238-246.

[8] J. W. Cho, and S. Jeon, and H. Y. Jeong: "Evaluation of cutting efficiency during TBM disc cutter excavation within a Korean granitic rock using linear-cutting-machine testing and photogrammetric measurement" Tunnelling and Underground Space Technology, Vol. 35, No. 2, 2013, pp.37-54., DOI: 10.1016 /j.tust.2012.08.006

[9] S. H. Chang, and S. W. Choi, and G. J. Bae: "Performance prediction of TBM disc cutting on granitic rock by the linear cutting test" Tunnelling and Underground Space Technology, Vol. 21, No. 3, 2006, pp.264-271., DOI:10.1016 /j.tust.2005. 12. 131

[10] H. Bejari, and K. Reza, and M. Ataei: "Simultaneous effects of joint spacing and joint orientation on the penetration rate of a single disc cutter" Mining Science and Technology, Vol. 21, No. 4, 2011, pp.507-512.

[11] H. Bejari, and H. J. Khademi: "Simultaneous Effects of Joint Spacing and Orientation on TBM Cutting Efficiency in Jointed Rock Masses" Rock Mechanics and Rock Engineering, Vol. 46, No. 4, 2012, pp.897-907., DOI: 10.1007 /s00603-012 -0314-2

[12] Q. M. Gong, and J. Zhao, and Y. Y. Jiao: "Numerical modeling of the effects of joint orientation on rock fragmentation by TBM cutters" Tunnelling and Underground Space Technology, Vol. 20, No. 2, 2005, pp.183-191., DOI: 10.1016 /j.tust.2004.08.006

[13] Q. M. Gong, and Y. Y. Jiao, and J. Zhao: "Numerical modelling of the effects of joint spacing on rock fragmentation by TBM cutters" Tunnelling and Underground Space Technology, Vol. 20, No. 1, 2006, pp.46-55., DOI: 10.1016 /j.tust.2004.08.006

[14] J. Liu, and P. Cao, and Du Chun: "Effects of discontinuities on penetration of TBM cutters" Journal of Central South University, Vol. 22, No. 9, 2015, pp.3624-3632.

[15] J. Liu, and P. Cao, and Z. Jiang: "Numerical simulation on effects of embedded crack on rock fragmentation by a tunnel boring machine cutter" Journal of Central South University, Vol. 21, No. 8, 2014, pp.3302-3308.

[16] J. S. Liu, and P. Cao, and J. Liu: "Influence of confining stress on fracture characteristics and cutting efficiency of TBM cutters conducted on soft and hard rock" Journal of Central South University, Vol. 22, No. 5,.2015, pp.1947-1955.

[17] J. Z. Huo, and W. Sun, and L. Guo: "Numerical simulation of the rock fracture process induced by multi-disc-cutters and cutter spacing design" Journal of Harbin Engineering University, Vol. 33, No. 1, 2012, pp.96-99.

[18] Z. Z. Liang, and Y. Yu, and S. B. Tang : "Numerical modeling of rock fracture mechanism under disc cutters and associated cutter spacing optimization" Journal of Mining & Safety Engineering, Vol. 29, No. 1, 2012, pp.84-90.

[19] Q. Tan, and N. E. Yi, and Y. M. Xia: "Study of calculation equation of TBM disc cutter optimal spacing" Rock and Soil Mechanics, Vol. 37, No. 3, 2016, pp.883-892., DOI:10.16285 /j.rsm.2016.03.034

Prof. TAN Qing , Address correspondence to TAN Qing at the State Key Laboratory of High Performance Complex Manufacturing, Central South University, Changsha, Hunan 410083, China;

YI Nian-en (Corresponding Author) is working on the rock breaking mechanics of TBM (tunnel boring machine) cutters and design problems. To improve the cutting performance and prolong cutter life. Address correspondence to corresponding author at the School of Mechanical and Electrical Engineering, Central South University, Changsha, Hunan 410083, China;